SEL-64-009

Studies of Microplasmas and High-Field Effects in Silicon

by
John L. Moll and Chun-Yuan Duh

1 February 1960 through 31 October 1963

FINAL REPORT

PREPARED UNDER
SIGNAL CORPS CONTRACT DA36(039)SC-85339

SOLID-STATE ELECTRONICS LABORATORY
STANFORD ELECTRONICS LABORATORIES
STANFORD UNIVERSITY · STANFORD, CALIFORNIA

SEL-64-009

STUDIES OF MICROPLASMAS AND HIGH-FIELD EFFECTS IN SILICON

by

John L. Moll and Chun-Yuan Duh

February 1964

FINAL REPORT

Prepared under
Signal Corps Contract DA 36-039 SC-85339

Solid-State Electronics Laboratory
Stanford Electronics Laboratories
Stanford University Stanford, California

ABSTRACT

This report contains a calculation of breakdown voltage for various types of junctions using the most recent and probably the most accurate measurements available for electron and hole ionization rates. In addition, there is a calculation of multiplication at voltages less than the breakdown voltage. This calculation is useful to obtain the BV_{CE} for n-p-n and p-n-p transistors. It is found that for similar collectors, the BV_{CE} for an n-p-n transistor is about half the value for a p-n-p transistor.

In addition to the multiplication calculations, there is included a discussion of previous work done on this contract, and an attempt to reconcile the discrepancy between the results of calculation of electron temperature at high and low fields. Inclusion of transverse acoustical phonon scattering results in a better fit of experiment and theory than just use of optical phonons and longitudinal acoustical phonons but there is still a significant discrepancy.

CONTENTS

ILLUSTRATIONS

SYMBOLS FOR APPENDIX

$a = \frac{\theta_a}{\theta_o}$

$B(q)_i$ = square of the interaction matrix element due to i^{th} mode of phonon

C = interaction constant of the order of a few ev

D = interaction constant of the order of a few to several tens ev

E_p = electron energy with momentum p

$\mathcal{E}(q)_i$ = phonon energy of i^{th} mode with momentum q, or associated with Debye temperature θ_i

e = electronic charge

$\vec{F}$ = applied electric field

h = Planck's constant

$\hbar = \frac{h}{2\pi}$

$\vec{j}$ = current density

$\vec{K}$ = a reciprocal lattice vector

k = Boltzmann's constant

ℓ_a = mean free path due to the scattering of low energy acoustic phonons

ℓ'_a = mean free path due to the scattering of transverse acoustic phonons near the zone edge

ℓ_i = mean free path due to the scattering of i^{th} mode of phonon

ℓ_o = mean free path due to the scattering of optical phonons at zone center

$M = \frac{\mu_{cA}}{b}$, reduced electron mobility

M' = ionic mass

m = effective electron mass

m_ℓ = longitudinal electron mass

m_o = electron mass

m_t = transverse electron mass

N = total number of electrons in the conduction band

N_a = number of transverse acoustic phonons on the zone edge

N_i = number of phonons of i^{th} mode

N_o = number of optical phonon at zone center

n_i = number of ions per unit volume

$P_i(\cos\theta)$ = Legendre polynomial of i^{th} order

$\vec{p}$ = electron momentum

p_o = momentum associated with electron drift

q = phonon momentum

q_o = greatest phonon momentum

$r = \frac{C^2}{18D^2}$, dimensionless constant of the order of a few times 10^{-2}

$R_1 = \frac{\theta^2}{4r\theta_o^2}$, adjustable parameter 1

$R_2 = \frac{\theta^2}{4r\theta_a^2}$, adjustable parameter 2

s = longitudinal sound velocity in the crystal

T = effective electron temperature

T_o = lattice temperature

ΔT = incremental change of electron temperature

V = crystal volume

$\vec{v}$ = drift velocity of the electron

$\alpha = \frac{\theta_a}{T}$

$\alpha_o = \frac{\theta_a}{T_o}$

$\gamma = \frac{\theta_o}{T}$

$\gamma_o = \frac{\theta_o}{T_o}$

$\delta = \frac{\Delta T}{T_o} \ll 1$

θ = Debye temperature of low energy acoustic phonons near zone center

θ_a = Debye temperature of transverse acoustic phonon near zone edge

θ_i = Debye temperature of i^{th} mode of phonon

θ_o = Debye temperature of optical phonons at zone center

θ_o' = Debye temperature of longitudinal optical phonon near zone edge

μ = effective electron mobility

μ_a = electron mobility due to low energy acoustic phonon

μ_a' = electron mobility due to transverse acoustic phonon near zone edge

μ_i = electron mobility due to i^{th} mode of phonon

μ_o = electron mobility due to optical phonon at zone center

μ_{aA} = zero field electron mobility due to low energy acoustic phonon

μ_{aA}' = zero field electron mobility due to transverse acoustic phonon near zone edge

μ_{cA} = zero field effective electron mobility

μ_{oA} = zero field electron mobility due to optical phonon at zone center

$\omega = \frac{\theta_i}{T}$

$\omega_o = \frac{\theta_i}{T_o}$

I. INTRODUCTION

This report is a final report on contract DA36(039)SC-85339. Some practical technological applications of studies of ionization rates in silicon are described: 1) prediction of breakdown voltage and capacitance, and junction width at breakdown for a variety of junctions, and 2) calculation of electron and hole multiplication rates at voltages less than the breakdown voltage. These calculations are useful in designing p-n junctions and junction transistors. A summary of other research that has been carried out on this contract is also included. The results of some of the studies have been published--in some cases they are in previous status reports. The significance of the work is discussed but the reporting is not repeated in detail. Also presented is a fairly extensive discussion (Appendix A) of a theoretical difficulty in relating the low-, intermediate-, and high-field behavior of charge carriers in silicon to each other. This problem is not resolved but we have attempted to clarify it.

II. BREAKDOWN VOLTAGE OF JUNCTIONS

One of the most practical objectives of measurements of ionization rates of electrons and holes in silicon is the prediction of breakdown voltage in various junctions. By breakdown voltage, we mean that voltage at which the junction will conduct a large amount of current with a trivial change in voltage. In silicon p-n junctions, there are enough data to calculate this voltage in a "perfect" junction. By a "perfect" junction we mean one that has no imperfections such as dislocations, precipitates, interstitial atoms, or vacancies in the high-field region. A perfect junction as defined does not exist, but there are surprisingly large numbers of commercial p-n junctions that approximate the perfect junction in breakdown properties. The result of intentionally introduced imperfections is generally to lower the breakdown field of a given p-n junction, resulting in some cases in a lower voltage and in some cases in a higher voltage. The theoretical possibility that the introduction of imperfections will increase the breakdown field cannot be entirely discounted.

Junction multiplication is defined as the ratio of total junction current to incident current. Thus, if there is an incident current of electrons only,

$$M_n = I/I_n. \tag{1}$$

Or, for an incident hole current

$$M_p = I/I_p. \tag{2}$$

Breakdown occurs when the multiplication values are infinite. By this definition, of course, a junction never reaches breakdown, but for practical purposes a breakdown voltage can be defined. The multiplication values reach infinity simultaneously; they are given by [Ref. 1]

$$M_n = \left\{ 1 - \exp \left[\int_o^w (\alpha_p - \alpha_n) dx \right] \int_o^w \alpha_n \exp \left[- \int_o^x (\alpha_p - \alpha_n) dx' \right] dx \right\}^{-1} \quad (3)$$

$$M_p = M_n \exp \left[\int_o^w (\alpha_p - \alpha_n) dx \right] \quad (4)$$

where

M_n, M_p = electron, hole multiplication

W = junction width

α_n, α_p = ionization rate for electrons, holes.

Junction breakdown occurs at

$$\int_o^w \alpha_n \exp \left[\int_x^w (\alpha_p - \alpha_n) dx' \right] dx = 1. \quad (5)$$

It is not possible to calculate the voltage at which Eq. (5) is satisfied for arbitrary variation of α_p, α_n without the aid of a computer. It is possible, however, to obtain a number that is within a few percent of the right voltage for many different types of junctions by using suitable approximations. It is found, for example, that in silicon, $\alpha_p \ll \alpha_n$. If a constant ratio is assumed for α_p/α_n, we obtain the condition

$$\int_o^w \alpha_n \exp \left[\int_x^w (\gamma - 1) \alpha_n dx' \right] dx = 1 \quad (6)$$

where $\alpha_p/\alpha_n = \gamma$ which is integrable for constant γ. The resulting condition for breakdown is

$$\int_o^w \alpha_n dx = \frac{\ell n\, \gamma}{\gamma - 1}. \quad (7)$$

Figure 1 is a plot of $\ln \gamma/\gamma\text{-}1$ vs γ. This function is a measure of the number of electron-hole pairs that an electron must produce in an average transit across the junction to maintain the breakdown discharge. For the 400/1 range of γ there is only a 10/1 range in the required number of electron-hole pairs produced by an average electron so that the actual value of breakdown voltage is fairly insensitive to the γ-parameter.

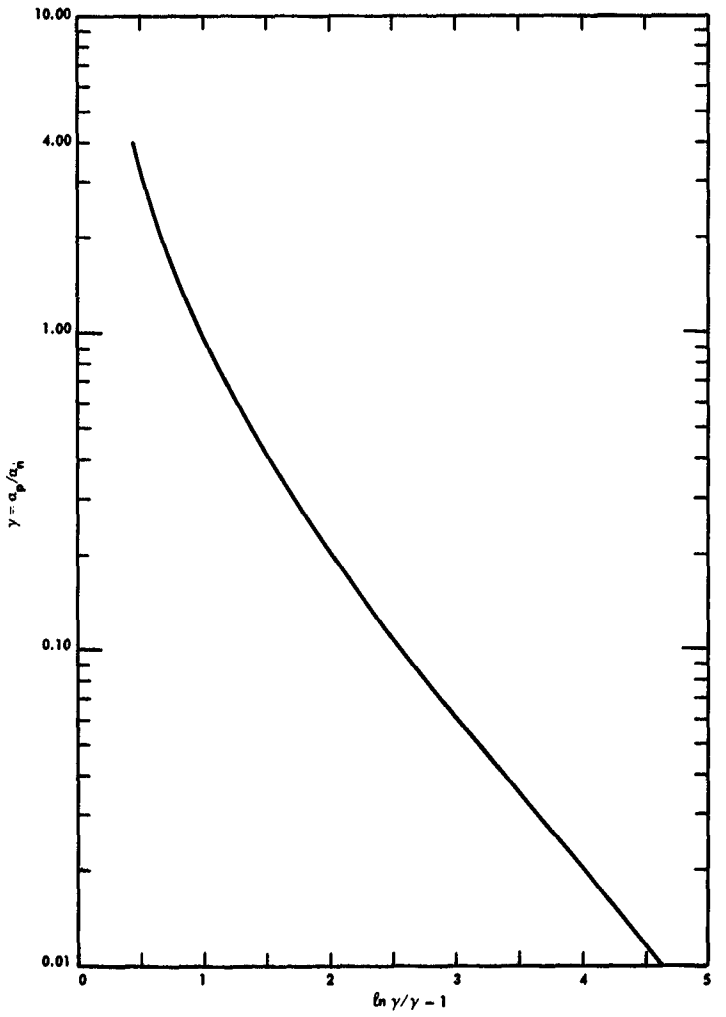

FIG. 1. ELECTRON IONIZATIONS PER TRANSIT AT BREAKDOWN ($\ell n\ \gamma/\gamma\text{-}1$) vs γ ($= \alpha_p/\alpha_n$)

Figure 2 shows measured values of ionization rate vs electric field for both electrons and holes [Ref. 2]. It is apparent from this figure that γ is a rapidly varying function of electric field. The variation of γ with electric field is not easily included in the breakdown relation [Eq. (6)] without the aid of a computer. An answer that is perfectly suitable for most purposes can be obtained for a variety of junctions by taking reasonable limits on γ in Eq. (7) and obtaining an upper and lower bound on the breakdown voltage. If the upper and lower limits are within a few percent of each other, the answer can be considered to be satisfactory.

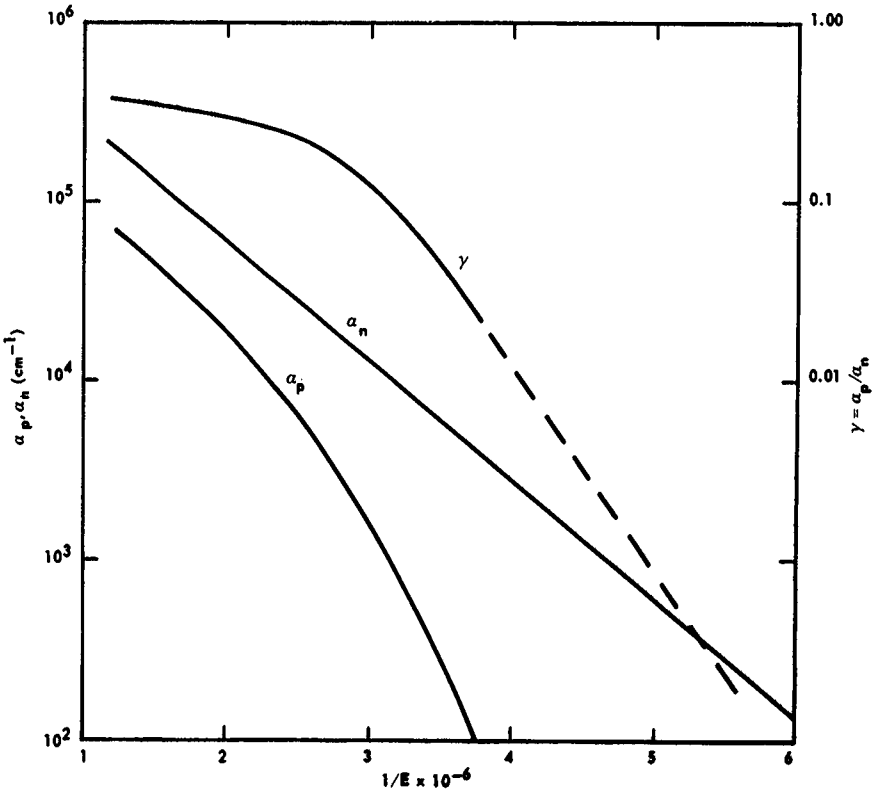

FIG. 2. IONIZATION COEFFICIENTS α_p, α_n, AND γ $(= \alpha_p/\alpha_n)$ VS RECIPROCAL FIELD. THE DASHED PART OF THE γ CURVE IS EXTRAPOLATED.

The electron ionization rate is reasonably well approximated by

$$\left.\begin{aligned} \alpha_n &\cong \alpha_\infty e^{-b/E} \\ \alpha_\infty &= 1.5\text{x}10^6 \text{ cm}^{-1} \\ b &= 1.6\text{x}10^6 \text{ v/cm.} \end{aligned}\right\} \quad (8)$$

It is relatively difficult to integrate the form of (8) in even such relatively simple junctions as graded and step junctions. These integrals have nevertheless been calculated and are [Ref. 3]

$$\int_0^W \alpha_n dx = \alpha_{max} W_{eff} , \quad (9)$$

where α_{max} is the ionization rate at the maximum field and W_{eff} has been calculated as shown in Fig. 3.

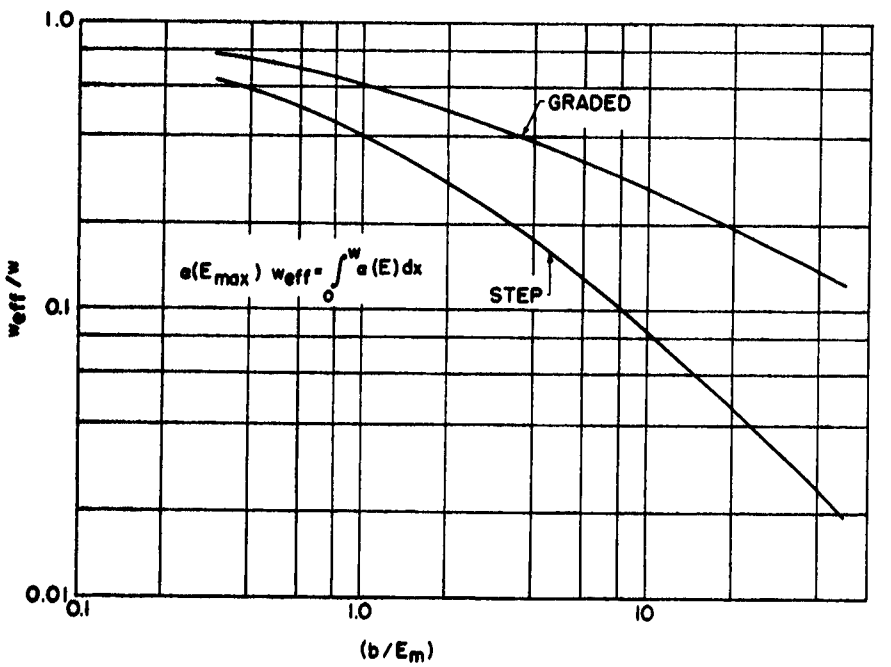

FIG. 3. PLOT OF W_{eff}/W VS b/E_m.

The procedure for calculating limits on breakdown voltage then is as follows. For example, consider the graded junction: choose $b/E_m = 4.0$. Then, from Fig. 3,

$$\frac{W_{eff}}{W} \cong 0.4 \qquad \text{and} \qquad \frac{1}{E_m} = 2.5\text{x}10^{-6}.$$

From Fig. 2,

$$\alpha_{max} = 2.8\text{x}10^{4} \qquad \text{and} \qquad \gamma(E_{max}) = 0.25.$$

From Fig. 1,

$$\alpha_m W_{eff} = 1.8$$

$$W_{eff} = 6.4\text{x}10^{-5}$$

$$W = 1.65\text{x}10^{-4}$$

$$V = 2/3\ E_m W = 45 \text{ v}.$$

The gradient for a junction that has a depletion-layer width of $1.65\text{x}10^{-4}$ cm at 45 v is obtained from standard p-n junction theory and is $8\text{x}10^{20}$ cm^{-4}. The electric field at a distance $\pm W_{eff}/2$ from the maximum field point is about 85 percent of the maximum field, at which γ is about 0.13. If this value of γ is used, we require

$$\alpha_m W_{eff} = 2.3$$

$$W_{eff} = 8.2\text{x}10^{-5}$$

$$W = 2.05\text{x}10^{-4} \text{ cm}$$

$$V = 2/3\ E_m W = 55 \text{ v}$$

$$a = 4.9\text{x}10^{20}.$$

The result of this calculation using a smaller value of γ is that the breakdown voltage for a given gradient should increase slightly. The use of the smaller value of γ is actually a slight over-estimate of the breakdown voltage since most of the ionization occurs in the distance W_{eff} near the high-field region. Since the procedure that we are using here results in different gradient and breakdown voltages, it is not possible to estimate the error introduced into the calculation of breakdown voltage by the assumption of constant γ from a single computation. The calculations of breakdown voltage vs gradient or impurity density are within about 1 percent of each other as determined by numerous computations and using the two extreme values of γ. We must conclude then that the constant-γ assumption does not introduce significant error into the calculation of junction breakdown. Figure 4 shows breakdown voltage as calculated by the above procedure for graded junctions. Figure 5 shows breakdown for step junctions and Fig. 6 shows the width at breakdown for graded, step, and PIN junctions. Use of the upper and lower bounds for γ result in a variance that is less than 2 percent for the entire range of breakdown that is shown. Figure 7 shows capacitance per unit area at breakdown for graded, step, and PIN junctions.

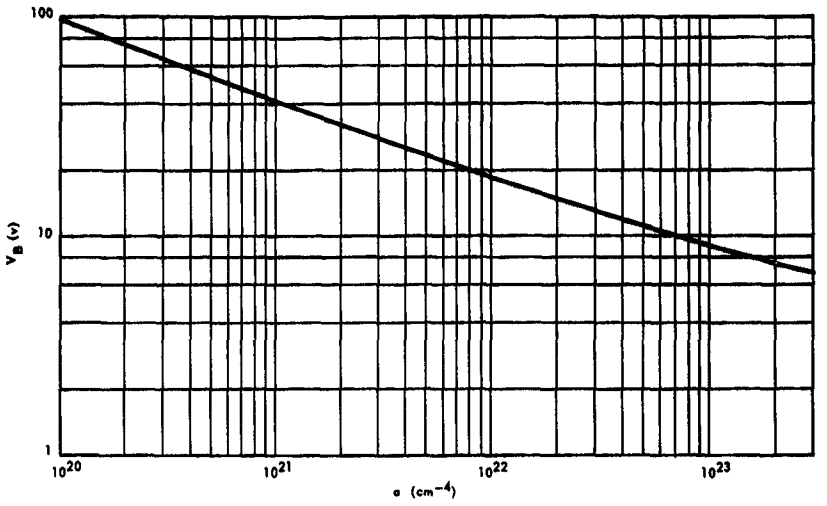

FIG. 4. BREAKDOWN VOLTAGE VS IMPURITY GRADIENT FOR LINEARLY GRADED JUNCTION.

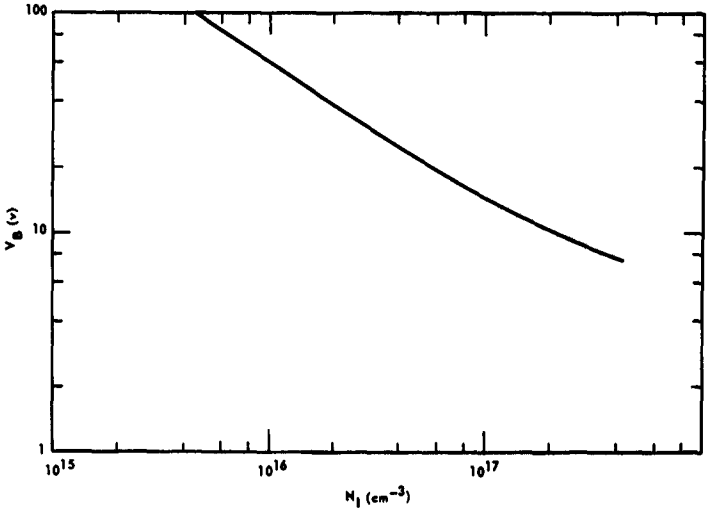

FIG. 5. BREAKDOWN VOLTAGE VS IMPURITY DENSITY FOR STEP JUNCTION.

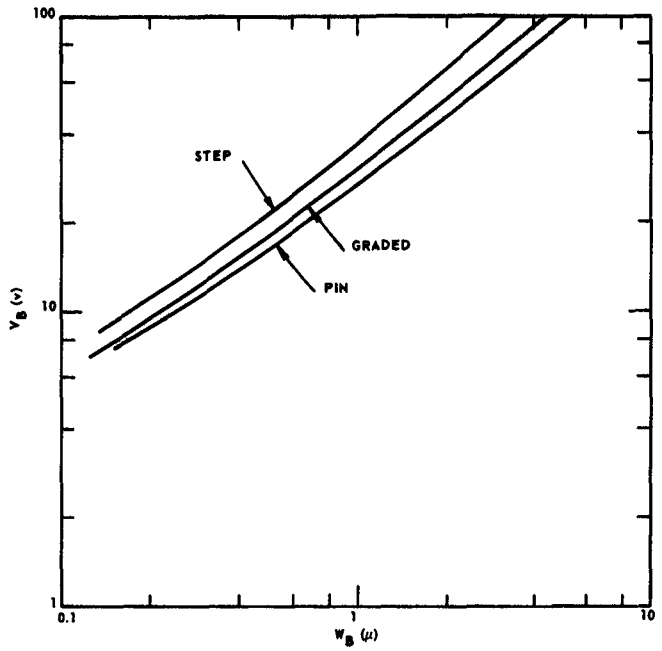

FIG. 6. JUNCTION WIDTH AT BREAKDOWN FOR A VARIETY OF IMPURITY PROFILES.

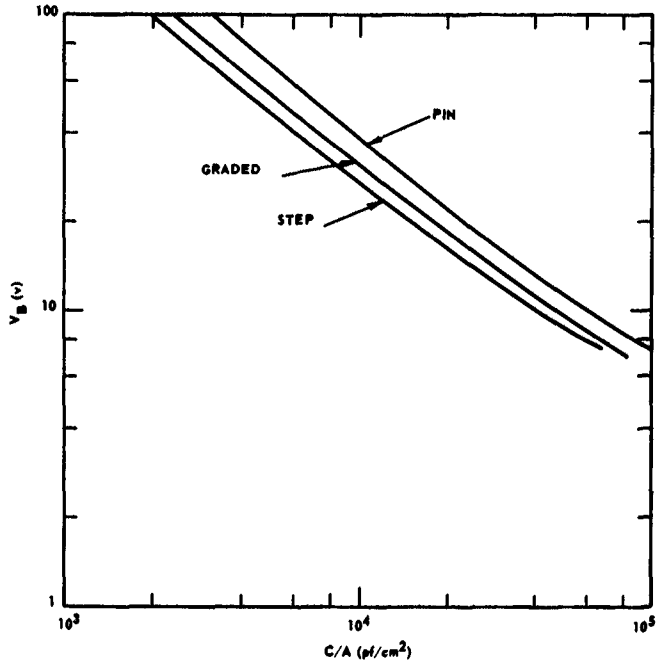

FIG. 7. CAPACITANCE PER UNIT AREA AT BREAKDOWN FOR A VARIETY OF IMPURITY PROFILES.

III. MULTIPLICATION IN TRANSISTOR COLLECTORS

At least as important as the breakdown voltage of a p-n junction is the amount of multiplication at voltages less than the breakdown voltage.

The switching response of a transistor is adversely affected if the collector voltage is sufficient to cause multiplication, and in some cases the transistor may become unstable if the product $\alpha_o M > 1$ where α_o is the low-voltage, small-signal alpha and M is the collector-multiplication factor. The maximum collector-emitter breakdown voltage is determined by the voltage at which $\alpha_o M = 1$

The multiplication at voltages less than the breakdown voltage can be calculated as a simple extension of the breakdown voltage. In the example of the breakdown calculation where the voltage at breakdown was 45 v, the width was 1.65 microns. The width at another voltage can be obtained from the fact that the width of a graded junction varies as the 1/3 power of voltage. Thus, at 30 v, for example,

$$W_{30} = 1.44\ \mu$$

$$1/E_{max} = 3.2 \times 10^{-6} \quad (= 2/3\ \frac{W}{V})$$

$$W_{eff}/w = 0.35$$

$$\alpha_{max} = 10^4$$

$$\alpha_{max}\ W_{eff} = 0.5$$

$$\gamma = 0.08$$

$$1 - \frac{1}{M_n} \cong \frac{1}{1-\gamma}\left\{1 - \exp\left[-(1-\gamma)\alpha_{max}\ W_{eff}\right]\right\}$$

$$\cong 0.36.$$

If γ_{min} is used where γ_{min} is the ratio of α_p/α_n at a distance $W_{eff}/2$ from the center of the junction, we obtain $1 - (1/M_n) \cong 0.40$ so that there is a 10-percent uncertainty in this calculation. To obtain the hole multiplication, it is most accurate to replace the electron-ionization-rate integral by one for holes. Thus

$$1 - \frac{1}{M_p} \cong \frac{1}{(1/\gamma) - 1} \left\{ \exp \left[\left(\frac{1}{\gamma} - 1 \right) \alpha_p \, W_{p\ eff} \right] - 1 \right\}$$

where $W_{p\ eff}$ is the effective width for hole ionization. As a rough approximation, we replace the hole ionization rate by

$$\alpha_p \cong 10^8 \exp \left[-3.7 \times 10^6 / E \right].$$

This is a reasonable approximation for reciprocal field greater than 2.7×10^{-6} and includes all junctions that have breakdown in excess of about 30 v. We do not have measurements of hole-ionization rate for electric field less than 2.7×10^5 v/cm ($1/E > 3.7 \times 10^{-6}$) at which field the ionization rate is about 100/cm. The ratio γ was extrapolated linearly to the low fields (i.e., less than 2.7×10^5 v/cm) as a basis for the calculations of electron-multiplication rate. The calculation of hole multiplication is similar to the electron calculation except that there is somewhat more uncertainty in the result. One expects that at very low values of multiplication, the value of $1 - 1/M_{n,p}$ should converge to

$$\int_0^W \alpha_{n,p} \, dx .$$

The large discrepancy between α_n and α_p requires that $1 - 1/M_n$ be less than about 0.2 and $1 - 1/M_p$ be less than 0.01 for reasonable equality to exist between the ionization integral and the multiplication functions. Figures 8 and 9 show $1 - 1/M_n$ and $1 - 1/M_p$ as a function of V/V_B for several breakdown values. As expected, the electron multiplication remains significant to much lower values of voltage than

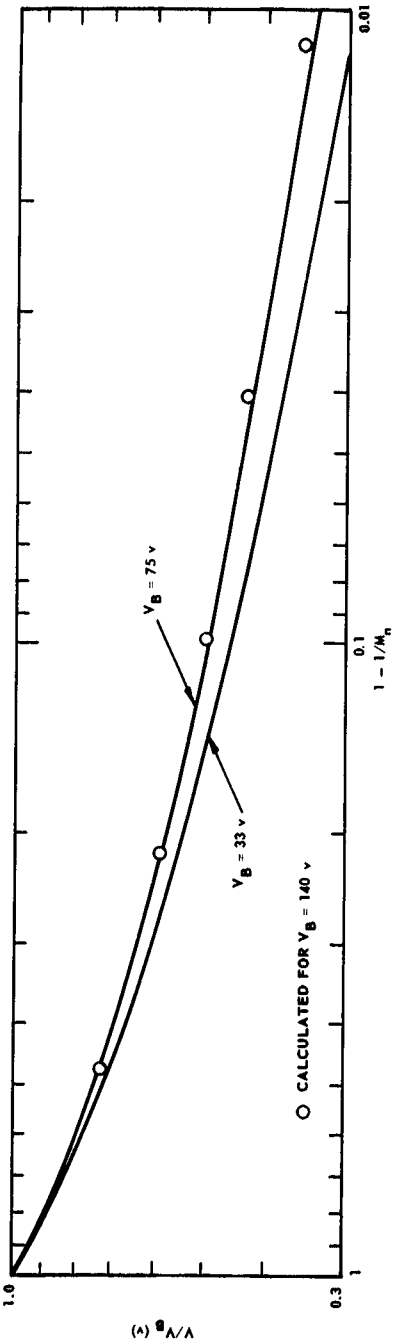

FIG. 8. ELECTRON MULTIPLICATION AS A FUNCTION OF V/V_B.

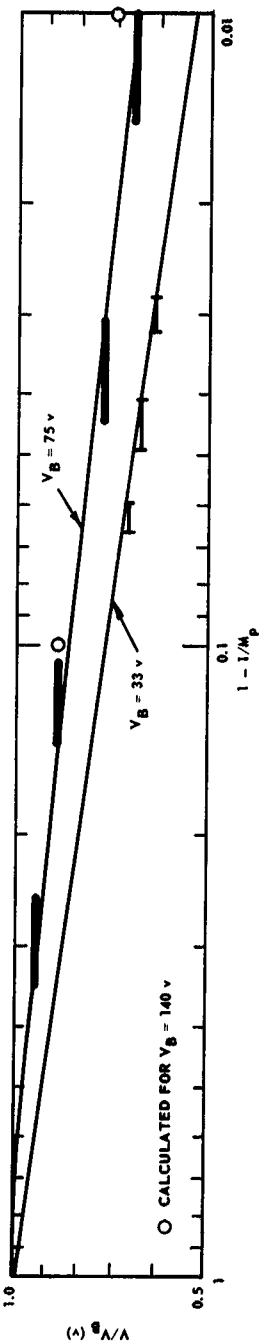

FIG. 9. HOLE MULTIPLICATION AS A FUNCTION OF V/V_B.

does hole multiplication. These figures can be used to calculate the collector-emitter breakdown voltage BV_{CE} for n-p-n and p-n-p transistors, respectively. The value of collector-emitter breakdown voltage BV_{CE} is obtained by finding the ratio $V/V_B = BV_{CE}/BV_{CB}$ that corresponds to $1 - 1/M = 1 - \alpha$ for the transistor in question. Thus a 75-v collector-base breakdown transistor with $1 - \alpha = 0.02$ will have $BV_{CE}/BV_{CB} = 0.38$ if it is n-p-n and $BV_{CE}/BV_{CB} = 0.70$ if it is p-n-p. The slow variation of the curves of Figs. 8 and 9 with breakdown voltage allows fairly wide application.

The fast variation of hole multiplication near the breakdown voltage also means that the uncertainty in determining the hole multiplication from the ionization rate is not a great disadvantage in the application of these curves to transistors. The mathematical simplicity that is gained from using the approximation of constant γ seems well warranted in light of these results.

IV. OTHER RESEARCH

A. MEASUREMENTS OF IONIZATION RATES

We have used both photo generation as well as electric emission of electrons and holes into silicon p-n junctions to measure ionization rates. The results of the ionization measurements are given in Fig. 2. It is not possible, in the arrangements we are using, to measure ionization rates of less than about 100/cm. To measure such low ionization rates, it would be necessary to construct junctions with breakdown voltage of the order of 500 - 1000 v and of the order of 50 microns thick. The ionization behavior of electrons and holes would be of interest to predict the multiplication behavior of high-voltage p-n junctions and to compare with theoretical calculations.

During the course of our measurements, a minor attempt was made to determine the effect of crystal imperfections on ionization rate. Within our experimental error, the ionization rates were not changed by neutron bombardment at the level of $10^{16}/cm^2$. These experiments were not sufficiently conclusive to be definitive.

B. MEASUREMENT OF ELECTRONS EMITTED INTO VACUUM

The number and energy distribution of electrons emitted into vacuum from a reverse-biased p-n junction is an important clue to mechanisms of energy loss by hot electrons. Fairly extensive work has been done in studying the emission of hot electrons across the silicon electron affinity of 3.8 ev into vacuum [Ref. 4]. This work has been analyzed quantitatively to give a simple model for the 4 - 5-v electron. Such an energetic electron has a lattice collision every 50-70 Å, giving up energy of the order of 0.06 ev (optical phonon energy), and has a collision with the valence electrons approximately every 200 Å, resulting in a secondary electron-hole pair. It must be emphasized that the behavior described here may not apply very well to the electrons that cause the actual secondaries in a p-n junction. We have shown that an electron requires a threshold energy of 1.8 ± 0.1 ev and a hole requires a threshold energy of 2.4 ± 0.1 ev to cause an ionization. It is the

nature of a threshold phenomenon that its probability increases rapidly near the threshold. Thus the ionization probability of electrons in the range 1.7 to 2 ev may be much less than one ionization for every 200 Å of travel.

An attempt was made to measure the electron emission and energy distribution with a very much lower surface barrier. A few layers of cesium on pure silicon can give a work function of the order of 1.5 ev. We prepared some junctions similar to the ones used in the study of vacuum emission across the silicon work function and obtained vacuum emission with only 2 v applied to the junction. It was not possible, however, to make the measurements that are analogous to the ones made with non-cesiated surfaces because the vacuum system tended to develop a shunt leakage path in the presence of the cesium vapor. The lack of success does not mean that the measurement cannot be made. The analysis of electron emission with cesium on the surface is an experiment that must be done with somewhat more extensive precautions to avoid leakage currents than we exercised. The results will be very interesting, as they will give a measure of ionization probability for electrons typical of those in an avalanching p-n junction.

C. THEORY

Theoretical considerations have been given for interpreting multiplication experiments, ionization thresholds, ionization rates [Refs. 3 - 5], and electron emission into vacuum. These considerations will not be repeated. A theoretical difficulty does exist in relating the theories of nonlinear mobility and the theories of ionization. These theories start at opposite ends of the electric-field range and must be extrapolated toward each other. If the extrapolations were within an order of magnitude in predicted electron temperature, we could be quite content that the phenomenon of hot electrons was well understood. Unfortunately, the work of Conwell [Ref. 6], and of Stratton [Ref. 7], who start at the low-field end, predicts electron temperatures of the order of 2000 to 3000 °K at electric fields of 2×10^4 v/cm. These electron temperatures are not obtained in the ionization theories of Shockley or Wolff until one reaches electric field of about 2×10^5 v/cm.

The electron temperature varies approximately as the square of electric field in the high-field range.

A brief description of the physical processes at the two ends of electric-field range will be given. In the Conwell and Stratton approach, it is supposed that electrons interact with long-wavelength acoustic phonons and with optical phonons. The optical-phonon energy is about 0.063 ev in silicon. The mobility associated with long-wavelength, acoustic-mode scattering has a $T^{-3/2}$ temperature dependence. The mobility associated with optical scattering has a much steeper dependence, since the optical phonon energy exceeds the value of kT/q in the range of interest. The actual temperature dependence is fitted by taking a mixture of acoustic and optical phonon scattering. This mixture is then used, as illustrated in the appendix, to calculate the field dependence of velocity. As the carriers heat up, the probability of optical-phonon interaction increases. A good fit to the velocity vs electric field is obtained up to fields of several thousand volts per centimeter.

In the ionization theory, it is assumed that all of the energy loss to the lattice is through optical-phonon collisions, and the mean free path for optical-phonon emission is adjusted to give the right amount of ionization. A value of 70 Å must be taken to fit the ionization data. This value results in much too low an electron temperature to be in agreement with the extrapolated low-field values even though it is in reasonable agreement with the spectrum of light emitted from avalanching p-n junctions.

There are several possible ways of resolving this discrepancy. As the electrons become more energetic, new scattering processes can set in. Thus, in silicon the <111> minima are about 0.39 ev above the <100> minima so that the density of end states is much greater for the more energetic electrons. It is also possible that the assumption of Maxwellian distribution is not valid at the very high fields.

Finally, it is necessary to consider the possibility of scattering by short-wavelength, transverse, acoustical phonons. There is a high density of states of such phonons, and their possible contribution to electron scattering has been ignored. This last possibility is the one that is most easily tested. The appendix gives details of a calculation,

following the method of Stratton, which includes the transverse acoustic phonon. The result of this inclusion is that it is possible to obtain a better fit to the velocity-vs-field curve than if such scattering is ignored. The electron temperature is reduced somewhat but is still too high. Our conclusion must be that further theoretical work is necessary to resolve this problem.

APPENDIX A. THEORETICAL VARIATION OF ELECTRON MOBILITY WITH EFFECTIVE ELECTRON TEMPERATURE AND APPLIED ELECTRIC FIELD IN SEMICONDUCTORS

1. Introduction

The theoretical variation of electron mobility with the applied field in semiconductors has been studied by several authors [Refs. 7, 8]. Shockley has calculated the variation of mobility with the applied field in covalent semiconductors assuming the lattice scattering is mainly due to the long-wavelength, acoustic phonons. His result is in reasonable agreement with room-temperature experiments on n-type germanium and silicon only up to 10^3 v/cm. This fact is verified by the experimental results given by Ryder [Ref. 9], Gunn [Ref. 10], and Gibson [Ref. 11]. Stratton has applied Fröhlich's and Paranjape's theory [Refs. 12, 13], assuming that the inter-electronic collisions essentially determine the distribution function, to derive the variation of electron mobility with applied field. In his formulations, he completely neglected the inter-valley scattering mechanism due to energetic phonons near the zone edge. Application of his result to n-type germanium is in good agreement with experimental data up to 3.5×10^3 v/cm. It is believed, however, that the corresponding electron temperature T is much higher than the actual situation.

The purpose of this report is to include the effect of the inter-valley scattering mechanism due to energetic phonons, both acoustic and optical. Ohm's law for electronic conductors is strictly obeyed only in the limit of vanishing applied electric field, when the electron gas and lattice vibrations are in quasi-thermal equilibrium. Application of an electric field raises the mean kinetic energy of the electrons, and the rate at which energy is supplied to the electrons by the field must be balanced by the rate at which energy is transferred from the electrons to the lattice by electron-phonon collisions. This is always true before avalanche breakdown occurs. If the increase of the mean kinetic energy is sufficiently large to make the electron gas become warm or even hot, the electron mobility will vary with the applied field and appreciable deviation from Ohm's law is expected to occur. The study

of a field-dependent electron temperature has been carried out by Fröhlich and Paranjape in considerable detail [Refs. 12, 13]. In the latter paper, Fröhlich and Paranjape have pointed out that, if the density of electrons is sufficiently high, one can assume that the energy and momentum transfers are controlled by inter-electronic collisions. The distribution function of the electrons in momentum space will then be in internal equilibrium at an effective electron temperature T that depends on the applied field F and is greater than the lattice temperature T_o. The whole distribution drifts in the direction of the applied field with a velocity equal to p_o/m.

We assume that the inter-electronic collisions essentially determine the electronic distribution function $f(\vec{p})$. Then the distribution must be a Maxwellian distribution that may be displaced in momentum space, i.e.,

$$f(\vec{p}) = A \exp\left(- \frac{|\vec{p}-\vec{p}_o|^2}{2mkT}\right), \qquad \int f(\vec{p})\, d^3\vec{p} = N, \tag{1.1A}$$

where the normalization constant A is independent of $\vec{p}$ but is determined by the total number of electrons N. With the form of the distribution function assumed, A is evaluated to be $N/(2\pi mkT)^{3/2}$. The distribution function $f(\vec{p})$ contains two parameters p_o and T, which will be determined from the rate of momentum and energy transfer to the lattice. If $f(\vec{p})$ is developed in spherical harmonics with the axis in the direction of the applied field, then it can be expanded as

$$f(\vec{p}) = f_o(\vec{p}) + f_1(\vec{p})\, P_1(\cos\theta) + \ldots \tag{1.2A}$$

where θ is the angle between $\vec{p}$ and the applied field $\vec{F}$, and

$$f_o(\vec{p}) \cong A \exp\left(- \frac{p^2}{2mkT}\right) \tag{1.3A}$$

$$f_1(p) = -p_o \frac{\partial f_o(p)}{\partial p} \cong \frac{pp_o}{mkT} f_o(p) \tag{1.4A}$$

when

$$\frac{p_o^2}{2mkT} \ll 1. \tag{1.5A}$$

Equation (1.5A) implies that the drift velocity is much less than the random thermal velocity. The current density $\vec{j}$ and the drift velocity $\vec{v}$ are related to $\vec{p}_o$ by

$$\vec{j} = Nev = Ne(\vec{p}_o/m), \tag{1.6A}$$

which, in turn, can be derived as functions of $\vec{F}$.

2. Calculation Assuming Inter-Electronic Collisions Predominate

The distribution function $f(\vec{p})$ in momentum space must satisfy the kinetic equation

$$\frac{\partial f}{\partial t} = \left(\frac{\partial f}{\partial t}\right)_F + \left(\frac{\partial f}{\partial t}\right)_L + \left(\frac{\partial f}{\partial t}\right)_e \tag{2.1A}$$

where the subscripts F, L and e respectively denote the rates of change of $f(\vec{p})$ due to an external field, to collisions with the lattice vibrations including both intra-valley and inter-valley scattering mechanisms, and to the inter-electronic collisions. In steady-state

$$\frac{\partial f}{\partial t} = 0. \tag{2.2A}$$

Since inter-electronic collisions conserve energy and momentum, it follows that

$$\sum_p \vec{p} \left(\frac{\partial f}{\partial t}\right)_e = 0, \qquad \text{and} \qquad \sum_p E_p \left(\frac{\partial f}{\partial t}\right)_e = 0 \tag{2.3A}$$

where

$$E_p = \frac{p^2}{2m} .$$

From Eqs. (2.1A) through (2.3A), we obtain

$$\sum_{\vec{p}} \vec{p} \left[\left(\frac{\partial f}{\partial t} \right)_F + \left(\frac{\partial f}{\partial t} \right)_L \right] = 0 \qquad (2.4A)$$

and

$$\sum_{\vec{p}} E_p \left[\left(\frac{\partial f}{\partial t} \right)_F + \left(\frac{\partial f}{\partial t} \right)_L \right] = 0. \qquad (2.5A)$$

Assuming the distribution function $f(\vec{p})$ is continuous in momentum space, it has been shown [Ref. 13] that

$$\int p_z \left(\frac{\partial f}{\partial t} \right)_F d^3\vec{p} = eFN \qquad (2.6A)$$

and

$$\int E_p \left(\frac{\partial f}{\partial t} \right)_F d^3\vec{p} = \frac{eFp_oN}{m} \qquad (2.7A)$$

where the field F is in the z direction. Equation (2.6A) is related to steady-state momentum of the electrons and Eq. (2.7A) is the rate of supplying energy from the electric field. Fröhlich and Paranjape have also considered the detailed processes of absorption and emission of phonons by electrons to calculate $(\partial f/\partial t)_L$. The result is

$$\left(\frac{\partial f}{\partial t} \right)_L \cong \sum_i [g_o(p)_i + p_o P_1 (\cos \theta)\, g_1(p)_i], \qquad (2.8A)$$

where

$$g_o(p)_i = -\frac{V}{2\pi\hbar^4}\frac{m}{p} f_o(p) \int q\, dq\, B(q)_i\, N_i$$

$$\left\{[1-\exp(\omega_o-\omega)]_+ + [\exp\omega_o-\exp\omega]_-\right\} \qquad (2.9A)$$

$$g_1(p)_i = -\frac{V}{2\pi\hbar^4}\frac{f_o(p)}{kT} \int q\, dq\, B(q)_i\, N_i \left\{\left[1-\left(1-\frac{q^2}{2p^2}+\frac{mk\theta_i}{p^2}\right)\exp(\omega_o-\omega)\right]_+\right.$$

$$\left. + \left[\exp\omega_o-\left(1-\frac{q^2}{2p^2}-\frac{mk\theta_i}{p^2}\right)\exp\omega\right]_-\right\} \qquad (2.10A)$$

and

$$\omega_o = \theta_i/T_o, \qquad \omega = \theta_i/T$$

where

T_o = lattice temperature

T = electron temperature.

The plus sign (+) outside the bracket indicates the term contributed from absorption of a phonon, and the minus sign (-) emission of a phonon. The subscript i corresponds to each mode of the vibrational phonons: $B(q)_i$ is the square of the interaction matrix element due to i^{th} mode, and the number of phonons corresponding to different modes is

$$N_i = \frac{1}{\exp(\omega_o)-1}, \qquad \mathcal{E}(q) = \hbar\,\omega(q) = k\theta_i. \qquad (2.11A)$$

Here $q/\hbar$ is the wave number of the phonons that scatter the electrons. From the vibrational spectra of covalent semiconductors Si and Ge [Refs. 14, 15] we expect that each of these modes will contribute both in the intra-valley and inter-valley scattering mechanisms. From Eqs. (2.4A)

through (2.8A) and making use of Eq. (1.6A), we obtain

$$jF = -\int E_p\left(\frac{\partial f}{\partial t}\right)_L d^3\vec{p} = -\int \frac{p^2}{2m} \sum_i g_o(p)_i d^3\vec{p}$$

$$= -\int E_p\left[\left(\frac{\partial f}{\partial t}\right)_a^{intra} + \left(\frac{\partial f}{\partial t}\right)_o^{intra} + \left(\frac{\partial f}{\partial t}\right)_{ta}^{inter} + \left(\frac{\partial f}{\partial t}\right)_{\ell o, \ell a}^{inter}\right] d^3\vec{p} \tag{2.12A}$$

$$eFN = -\int p_z \left(\frac{\partial f}{\partial t}\right)_L d^3\vec{p} = -\frac{p_o}{3} \int p \sum_i g_1(p)_i d^3\vec{p}$$

$$= -\int p_z\left[\left(\frac{\partial f}{\partial t}\right)_a^{intra} + \left(\frac{\partial f}{\partial t}\right)_o^{intra} + \left(\frac{\partial f}{\partial t}\right)_{ta}^{inter} + \left(\frac{\partial f}{\partial t}\right)_{\ell o, \ell a}^{inter}\right] d^3\vec{p} \tag{2.13A}$$

Here we use the property of orthogonality relation for Legendre polynomials; only the zero-order term $P_o(\cos\theta)$ contributes to the energy integral, while the first-order term $P_1(\cos\theta)$ contributes only to the momentum integral. The superscripts stand for different modes of the phonons.

The upper and lower limits of integration for q in Eqs. (2.9A) and (2.10A) are found to be [Ref. 13]

$$q_{\pm u} = p + (p^2 \pm 2mk\theta_i)^{1/2}\, U(p^2 \pm 2mk\theta_i) \tag{2.14A}$$

$$q_{\pm \ell} = p - (p^2 \pm 2mk\theta_i)^{1/2}\, U(p^2 \pm 2mk\theta_i) \tag{2.15A}$$

for the bracket marked + and - respectively. $U(x)$ is equivalent to a unit step function that is zero when x is negative and unity when x is positive. The θ_i are the equivalent Debye temperatures corresponding to different modes of the phonon both at zone center and near the zone edge in the reduced Brillouin zone representation.

For intra-valley scattering of low-energy, long-wavelength, acoustic phonons, the upper and lower integration limits of Eqs. (2.9A) and (2.10A) should be $2p$ and 0 respectively. Since we know from the vibrational spectra and the order of magnitude of the mean electron energy that $q_o > 2p$, after simple calculation we have

$$g_o(p)_a^{intra} = - \frac{f_o(p)}{p} \frac{4p^2}{4mkT_o \ell_a} \left(\frac{1}{kT} - \frac{T_o}{kT^2} \right) \tag{2.16A}$$

$$g_1(p)_a^{intra} = - \frac{f_o(p)}{mkT} \frac{1}{4m\ell_a} \left\{ 4p^2 + s \frac{16p^3}{5kT_o} + s^2 \left[\frac{4mp^2}{k} \left(\frac{2}{T} - \frac{1}{T_o} \right) \right.\right.$$

$$\left.\left. + \frac{32mp^3}{5k^2T_o} \left(\frac{1}{T} - \frac{1}{2T_o} \right) + \frac{4p^4}{3k^2} \left\{ \frac{2}{T_o^2} + \frac{4}{T} \left(\frac{1}{T} - \frac{1}{T_o} \right) \right\} \right] \right\}. \tag{2.17A}$$

Here we make use of the relations [Refs. 13, 16]

$$\left.\begin{aligned} B(q)_a^{intra} &= \frac{2C^2q}{9M's\ V\ n_i} \qquad \mathcal{E}(q) = qs \\ q_o &= \hbar(6\pi^2 n_i)^{1/3} \\ \ell_a &= \frac{3}{8\pi} \frac{\hbar M's^2 q_o^3}{C^2 m^2 kT_o} \end{aligned}\right\} \tag{2.18A}$$

and

$$\frac{V}{2\pi h^4} mB(q)_a^{intra} = \frac{\mathcal{E}(q)}{4mkT_o \ell_a} .$$

Now, from Eqs. (2.16A) and (2.17A), and applying the relation of (2.8A) into Eqs. (2.12A) and (2.13A), we obtain

$$-\int E_p \left(\frac{\partial f}{\partial t} \right)_a^{intra} d^3\vec{p} = Ne \frac{32s^2}{\pi\mu_a} \left(\frac{T}{T_o} \right)^{3/2} \left(1 - \frac{T_o}{T} \right) \tag{2.19A}$$

$$-\int p_z \left(\frac{\partial f}{\partial t}\right)_a^{\text{intra}} d^3\vec{p} \cong Nev\left[\frac{32}{9\pi\mu_a}\left(\frac{T}{T_o}\right)^{1/2} + \frac{16s\Gamma\left(\frac{7}{2}\right)}{45\sqrt{2}\ \pi\mu_a}\left(\frac{m}{kT}\right)^{1/2}\left(\frac{T}{T_o}\right)^{3/2}\right] \quad (2.20A)$$

where

$$\mu_a = \frac{4e\ell_a}{3(2\pi mkT_o)^{1/2}} .$$

In calculating the result of Eq. (2.20A), we retain only up to the first order of s in Eq. (2.17A). The ratio of the second term to the first term in the right-hand side of Eq. (2.20A) is of the order of 10^{-4} at room temperature for covalent semiconductors Si and Ge. Thus the second term is completely negligible.

In order to calculate the effects that come from inter-valley scattering near the zone edges, we assume that the scattering mechanisms due to the energetic phonons either at the zone center or on the zone edge are of the same form. Then we may substitute the upper and lower limits of integration from Eqs. (2.14A) and (2.15A) into Eqs. (2.9A) and (2.10A), also making use of the relations [Refs. 16, 17]

$$\left.\begin{aligned} B(q)_i &= \frac{\hbar^2 D^2 K^2}{2n_i M' V k\theta_i}, \qquad \mathcal{E}(q)_i = k\theta_i \\ q_o &= \hbar(6\pi^2 n_i)^{1/3} \\ \ell_i &= \frac{1}{6\pi(2N_i+1)} \frac{\hbar M' k\theta_i q_o^3}{D^2 m^3 (h^2K^2/2m)} \end{aligned}\right\} \quad (2.21A)$$

and

$$\frac{V}{2\pi\hbar^4} m^2 B(q)_i = \frac{1}{2(2N_i+1)\ell_i}$$

to obtain

$$g_o(p)_i = \frac{f_o(p)}{p} \frac{2E_p}{(2N_i+1)} [(N_i+1)e^{-\omega} - N_i] \left[\left(1+\frac{k\theta_i}{E}\right)^{1/2} - \left(1-\frac{k\theta_i}{E}\right)^{1/2} U\left(1-\frac{k\theta_i}{E}\right)e^{\omega}\right] \tag{2.22A}$$

$$g_1(p)_i = -\frac{p}{mkT}\frac{f_o(p)}{\tau_i(E)} = -\frac{f(E)}{\tau_i(E)} \tag{2.23A}$$

where

$$\frac{1}{\tau_i(E)} = \frac{(2E/m)^{1/2}}{\ell_i} \frac{N_i[1+(k\theta_i/E)]^{1/2} + (N_i+1)[1-(k\theta_i/E)]^{1/2} U[1-(k\theta_i/E)]}{2N_i+1}. \tag{2.24A}$$

Again carrying out the energy and the momentum integrals using Eqs. (2.12A) and (2.13A), we obtain

$$-\int E_p \left(\frac{\partial f}{\partial t}\right)_i d^3\vec{p} = Ne \frac{8}{3\pi} \frac{k\theta_i}{m\mu_i(2N_i+1)} \left(\frac{T}{T_o}\right)^{1/2} [(N_i+1)\, e^{-\omega} - N_i]\, J_o(\omega) \tag{2.25A}$$

$$-\int p_z \left(\frac{\partial f}{\partial t}\right)_i d^3\vec{p} = Nev \frac{16}{9\pi} \frac{1}{(2N_i+1)\mu_i} \left(\frac{T}{T_o}\right)^{1/2} \{[(N_i+1)\, e^{-\omega} + N_i]\, J_1(\omega) + \omega\, J_o(\omega)\, (N_i+1)\, e^{-\omega}\} \tag{2.26A}$$

where

$$\mu_i = \frac{4e\ell_i}{3(2\pi mkT_o)^{1/2}}.$$

$J_1(\omega)$ and $J_o(\omega)$ are two integrals that can be evaluated in terms of modified Bessel functions of the second kind* as

*We would like to thank Professor G. E. Latta who helped us evaluate the integrals in exact forms.

$$J_o(\omega) = \int_o^\infty e^{-x}[x(x+\omega)]^{1/2}\, dx = \frac{\omega}{2} \exp(\frac{\omega}{2})\ K_1(\frac{\omega}{2})$$

$$J_1(\omega) = \int_o^\infty e^{-x}[x^3(x+\omega)]^{1/2}\, dx \qquad (2.27A)$$

$$= \omega \exp(\frac{\omega}{2})\{K_1(\frac{\omega}{2}) - \frac{\omega}{4}\,[K_1(\frac{\omega}{2}) - K_o(\frac{\omega}{2})]\}$$

Now, combine all the individual terms in Eqs. (2.12A) and (2.13A) together, lumping the terms due to optical phonons into one term with a weighting factor of 1.7. Since $\theta_o' \cong 0.8\theta_o$, detailed analysis shows that this factor is quite reasonable. Actually, the weighting factor here is not important at all since there are still some adjustable parameters in the final results that should be determined from the temperature dependence of the measured electron-mobility data. However, it does indicate the physical picture implied in the formulations. The final results are

$$vF = \frac{32s^2}{\pi\mu_a}\left(\frac{T}{T_o}\right)^{3/2}\left(1-\frac{T_o}{T}\right) + \frac{8}{3\pi}\frac{k\theta_a}{m\mu_a'(2N_a+1)}\left(\frac{T}{T_o}\right)^{1/2}[(N_a+1)\ e^{-\alpha} - N_a]\ J_o(\alpha)$$

$$+ \frac{8}{3\pi}\frac{1.7\ k\theta_o}{m\mu_o(2N_o+1)}\left(\frac{T}{T_o}\right)^{1/2}[(N_o+1)\ e^{-\gamma} - N_o]\ J_o(\gamma) \qquad (2.28A)$$

$$\frac{F}{v} = \frac{32}{9\pi\mu_a}\left(\frac{T}{T_o}\right)^{1/2} + \frac{16}{9\pi}\frac{1}{(2N_a+1)\mu_a'}\left(\frac{T}{T_o}\right)^{1/2}\{[(N_a+1)\ e^{-\alpha}+N_a]\ J_1(\alpha) + \alpha J_o(\alpha)$$

$$(N_a+1)\ e^{-\alpha}\} + \frac{16}{9\pi}\frac{1.7}{(2N_o+1)\mu_o}\left(\frac{T}{T_o}\right)^{1/2}\{[(N_o+1)\ e^{-\gamma} + N_o]\ J_1(\gamma)$$

$$+ \gamma J_o(\gamma)\ (N_o+1)\ e^{-\gamma}\}. \qquad (2.29A)$$

The field dependence of the drift velocity v can be evaluated from these results if we can eliminate the effective electron temperature T between Eqs. (2.28A) and (2.29A). Three special cases of zero, very weak, and very strong applied fields, will be considered in more detail:

a. For the Zero-Field Case

In the limit of vanishing applied field, the mobility is given by

$$\frac{1}{\mu_{cA}} = \lim_{F\to 0}\left(\frac{F}{v}\right) = \frac{1}{\mu_{aA}} + \frac{1}{\mu'_{aA}} + \frac{1}{\mu_{oA}} \tag{2.30A}$$

where

$$\left.\begin{aligned} \mu_{aA} &= \frac{9\pi}{32}\,\mu_a \\ \mu'_{aA} &= \frac{9\pi\mu'_a}{32}\,\frac{2N_a+1}{N_a[J_1(\alpha_o)+(\alpha_o/2)J_o(\alpha_o)]} \\ \mu_{oA} &= \frac{9\pi\mu_o}{32}\,\frac{2N_o+1}{1.7N_o[J_1(\gamma_o)+(\gamma_o/2)J_o(\gamma_o)]}\,. \end{aligned}\right\} \tag{2.31A}$$

Substituting the relations of Eq. (2.31A) back into Eqs. (2.28A) and (2.29A) leads to

$$vF = \frac{9s^2}{\mu_{aA}}\left(\frac{T}{T_o}\right)^{3/2}\left(1-\frac{T_o}{T}\right) + \frac{3k\theta_a}{4m\mu'_{aA}}\,J_o(\alpha)\left(\frac{T}{T_o}\right)^{1/2}[(N_a+1)e^{-\alpha}-N_a]$$

$$\{N_a[J_1(\alpha_o)+(\alpha_o/2)J_o(\alpha_o)]\}^{-1} + \frac{3k\theta_o}{4m\mu_{oA}}\,J_o(\gamma)\left(\frac{T}{T_o}\right)^{1/2}[(N_o+1)e^{-\gamma}-N_o]$$

$$\{N_o[J_1(\gamma_o)+(\gamma_o/2)J_o(\gamma_o)]\}^{-1} \tag{2.32A}$$

$$\frac{F}{v} = \frac{1}{\mu_{aA}}\left(\frac{T}{T_o}\right)^{1/2} + \frac{1}{\mu'_{aA}}\left(\frac{T}{T_o}\right)^{1/2}\{[(N_a+1)e^{-\alpha}+N_a]J_1(\alpha)+\alpha J_o(\alpha)(N_a+1)e^{-\alpha}\}$$

$$\{2N_a[J_1(\alpha_o)+(\alpha_o/2)J_o(\alpha_o)]\}^{-1} + \frac{1}{\mu_{oA}}\left(\frac{T}{T_o}\right)^{1/2}\{[(N_o+1)e^{-\gamma}+N_o]J_1(\gamma)$$

$$+\gamma J_o(\gamma)(N_o+1)e^{-\gamma}\}\{2N_o[J_1(\gamma_o)+(\gamma_o/2)J_o(\gamma_o)]\}^{-1} . \qquad (2.33A)$$

The variation of the zero field mobility μ_{cA} with the lattice temperature will be considered as follows. Since ℓ_a is inversely proportional to T_o, μ_{aA} can therefore be written as

$$\mu_{aA} = b(\gamma_o)^{3/2} \qquad (2.34A)$$

where

$$b = \frac{3\pi}{8}\frac{e}{\theta_o^{3/2}}\frac{1}{(2\pi mk)^{1/2}} \quad \text{constant.}$$

Furthermore, from Eqs. (2.21A), also using the relations $\hbar K/2 \cong q_o$ and $q_o s \cong k\theta$, where θ is the corresponding Debye temperature of the low-energy acoustic phonons near zone center, we may derive the following relations

$$\frac{\ell_a}{\ell'_a} = \frac{1}{4r}\frac{(2N_a+1)\theta^2}{T_o\theta_a} \qquad (2.35A)$$

$$\frac{\ell_a}{\ell_o} = \frac{1}{4r}\frac{(2N_o+1)\theta^2}{T_o\theta_o} \qquad (2.36A)$$

where $r = C^2/18D^2$ is a dimensionless constant of the order of a few hundredths [Refs. 16, 18]. Therefore, we have, from Eq. (2.31A),

$$\mu'_{aA} = b(\gamma_o)^{1/2} \frac{4r\theta_a^2}{a\theta^2} \{N_a[J_o(\alpha_o)+(\alpha_o/2)J_o(\alpha_o)]\}^{-1} \qquad (2.37A)$$

$$\mu_{oA} = b(\gamma_o)^{1/2} \frac{4r\theta_o^2}{\theta^2} \{N_o[J_1(\gamma_o)+(\gamma_o/2)J_o(\gamma_o)]\}^{-1} \qquad (2.38A)$$

where

$$a = \frac{\theta_a}{\theta_o} .$$

If we introduce the reduced quantities

$$M = \frac{\mu_{cA}}{b}, \qquad R_1 = \frac{\theta^2}{4r\theta_o^2}, \qquad R_2 = \frac{\theta^2}{4r\theta_a^2} \qquad (2.39A)$$

and substitute them into Eq.(2.30A), we obtain

$$\frac{1}{M} = (\gamma_o)^{-3/2} + \frac{aR_2[J_1(a\gamma_o)+(a\gamma_o/2)J_o(a\gamma_o)]}{(\gamma_o)^{1/2}(e^{a\gamma_o}-1)} + \frac{1.7R_1[J_1(\gamma_o)+(\gamma_o/2)J_o(\gamma_o)]}{(\gamma_o)^{1/2}(e^{\gamma_o}-1)} \qquad (2.40A)$$

The plots of M vs $1/\gamma_o$ for two extreme cases are given in Figs. 10 a and b. One extreme case, which is $R_2 = 0$ and R_1 adjustable, is equivalent to Herring's result [Ref. 19].

b. For the Very Weak Field Case

We may assume that $T = T_o + \Delta T$, and expanding Eqs. (2.32A) and (2.33A) in power series of $\delta = \Delta T/T_o \ll 1$, retaining up to the first order of δ, we thus eliminate δ between the two equations. We then solve v in terms of F. The result gives

$$\mu = \mu_{cA}\left(1-\frac{F^2}{F_1^2}\right) \qquad (2.41A)$$

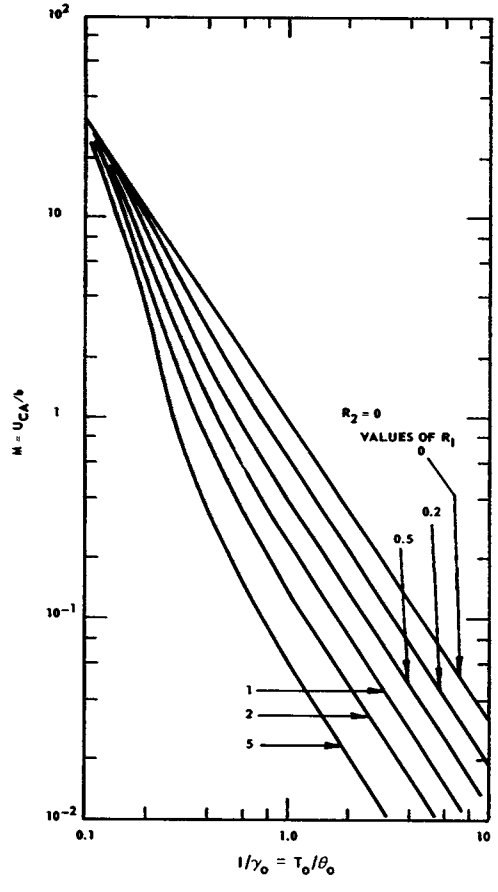

a. For the case $R_2 = 0$, and R_1 adjustable

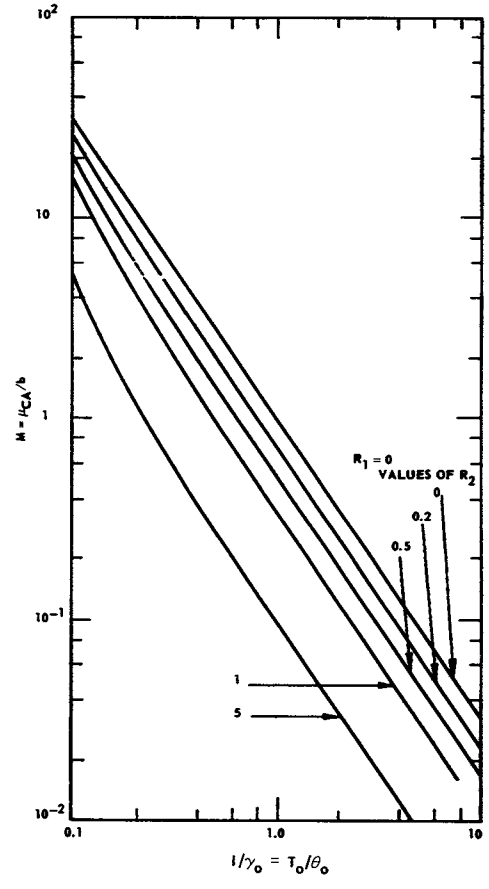

b. For the case $R_1 = 0$, and R_2 adjustable

FIG. 10. PLOT OF THE REDUCED ZERO-FIELD MOBILITY-TEMPERATURE CURVES ACCORDING TO EQ. (2.40A).

where

$$F_1^2 = \frac{1}{\mu_{cA}^2}\left\{18s^2+\frac{3k\theta_a}{2m}\frac{\mu_{aA}}{\mu'_{aA}}\frac{\alpha_o J_o(\alpha_o)}{J_1(\alpha_o)+(\alpha_o/2)J_o(\alpha_o)}\right.$$
$$\left.+\frac{3k\theta_o}{2m}\frac{\mu_{aA}}{\mu_{oA}}\frac{\gamma_o J_o(\gamma_o)}{J_1(\gamma_o)+(\gamma_o/2)J_o(\gamma_o)}\right\}\left\{1+\frac{\mu_{aA}}{\mu'_{aA}}\left[1+\frac{\alpha_o J_1(\alpha_o)+\alpha_o(\alpha_o-1)J_o(\alpha_o)}{J_1(\alpha_o)+(\alpha_o/2)J_o(\alpha_o)}\right]\right.$$
$$\left.+\frac{\mu_{aA}}{\mu_{oA}}\left[1+\frac{\gamma_o J_1(\gamma_o)+\gamma_o(\gamma_o-1)J_o(\gamma_o)}{J_1(\gamma_o)+(\gamma_o/2)J_o(\gamma_o)}\right]\right\}^{-1}. \qquad (2.42A)$$

c. For a Very Strong Field Case

If the applied field is sufficiently strong to make $T \gg \theta_o$ and $T \gg \theta_a$, i.e., $\gamma \ll 1$, $\alpha \ll 1$, then Eqs. (2.28A) and (2.29A) reduce to

$$vF \cong \frac{8}{\pi}\left[\frac{4s^2}{\mu_a}\left(\frac{T}{T_o}\right)^{3/2}+\frac{k\theta_a}{3m\mu'_a(2N_a+1)}\left(\frac{T}{T_o}\right)^{1/2}+\frac{1.7k\theta_o}{3m\mu_o(2N_o+1)}\left(\frac{T}{T_o}\right)^{1/2}\right] \qquad (2.43A)$$

$$\frac{F}{v} \cong \frac{32}{9\pi}\left(\frac{1}{\mu_a}+\frac{1}{\mu'_a}+\frac{1.7}{\mu_o}\right)\left(\frac{T}{T_o}\right)^{1/2}. \qquad (2.44A)$$

The best fit of the calculation to the experimental data of n-type silicon, suggests that the third term in the right-hand side of Eq. (2.43A) dominates almost all the way through the applied field range before breakdown occurs. (The same also occurs for n-type germanium, which is not presented in this report). Therefore, we are unable to get $F^{1/2}$ dependence of the drift velocity v at high field, which is true only when the first term in the right-hand side of Eq. (2.43A) predominates. We do get the result that the theoretical fitted curve almost comes to saturation at high field range.

3. Application of the Results to n-Type Silicon

The band structure of silicon based on a quantum-theoretical calculation, has been successfully carried out by F. Herman [Ref. 20]

and D. P. Jenkins [Ref. 21]. The conduction band of Si has six equivalent minima, which occur at points lying in the <100> directions and having values of $\vec{K}$ equal to about $0.8\,\vec{K}_{max}$, where $\vec{K}_{max}$ is the value of $\vec{K}$ corresponding to the zone boundary in these directions. The effective mass of electrons in the conduction band, which is actually associated with variation, is assumed constant in the fitting process. Its value is calculated from the relation

$$\frac{1}{m} = \frac{1}{3}\left(\frac{2}{m_t} + \frac{1}{m_\ell}\right). \tag{3.1A}$$

Substituting the values $m_t = 0.19\ m_o$, $m_\ell = 0.98\ m_o$ [Ref. 22], we obtain $m = 0.26\ m_o$. The sound velocity in n-type silicon can be evaluated by comparing the vibrational spectra of Ge and Si [Refs.14,15] and also by making use of the sound velocity of 5.4x10 cm/sec in Ge [Refs. 8, 23] to give $s = 7.05\text{x}10^5$ cm/sec. The effective Debye temperatures corresponding to the optical phonons at zone center and transverse acoustic phonons near zone edge can be evaluated from the vibrational spectra [Ref. 14]. The results are $\theta_o \cong 690\ ^\circ K$ and $\theta_a \cong 200\ ^\circ K$. The experimental result of n-type silicon given by Ludwig [Ref. 24] will be used to fit the temperature dependence of the zero field mobility. Applying their result yields

$$\mu_{cA} = 2.1\text{x}10^9\ T_o^{-2.5}\ \text{cm}^2/\text{v-sec}. \tag{3.2A}$$

If $150\ ^\circ K \leqq T_o \leqq 350\ ^\circ K$, graphical analysis shows that $T_o^{-2.5}$ dependence can be fitted to within ±10 percent with the best fit of the field dependence of drift velocity v. The final result is shown in Fig. 11 with $R_1 = 1.5$ and $R_2 = 1.5$ that leads to

$$\mu_{aA} = 3.16\text{x}10^3 \left(\frac{690}{T_o}\right)^{3/2} \text{cm}^2/\text{v-sec} \tag{3.3A}$$

$$\mu'_{aA} = 7.26\text{x}10^3 \left(\frac{690}{T_o}\right)^{1/2} \frac{\exp(200/T_o) - 1}{J_1(200/T_o) + (100/T_o)\ J_o(200/T_o)}\ \text{cm}^2/\text{v-sec}$$

$$\mu_{oA} = 1.24\text{x}10^3 \left(\frac{690}{T_o}\right)^{1/2} \frac{\exp(690/T_o) - 1}{J_1(690/T_o) + (345/T_o)\ J_o(690/T_o)}\ \text{cm}^2/\text{v-sec}.$$

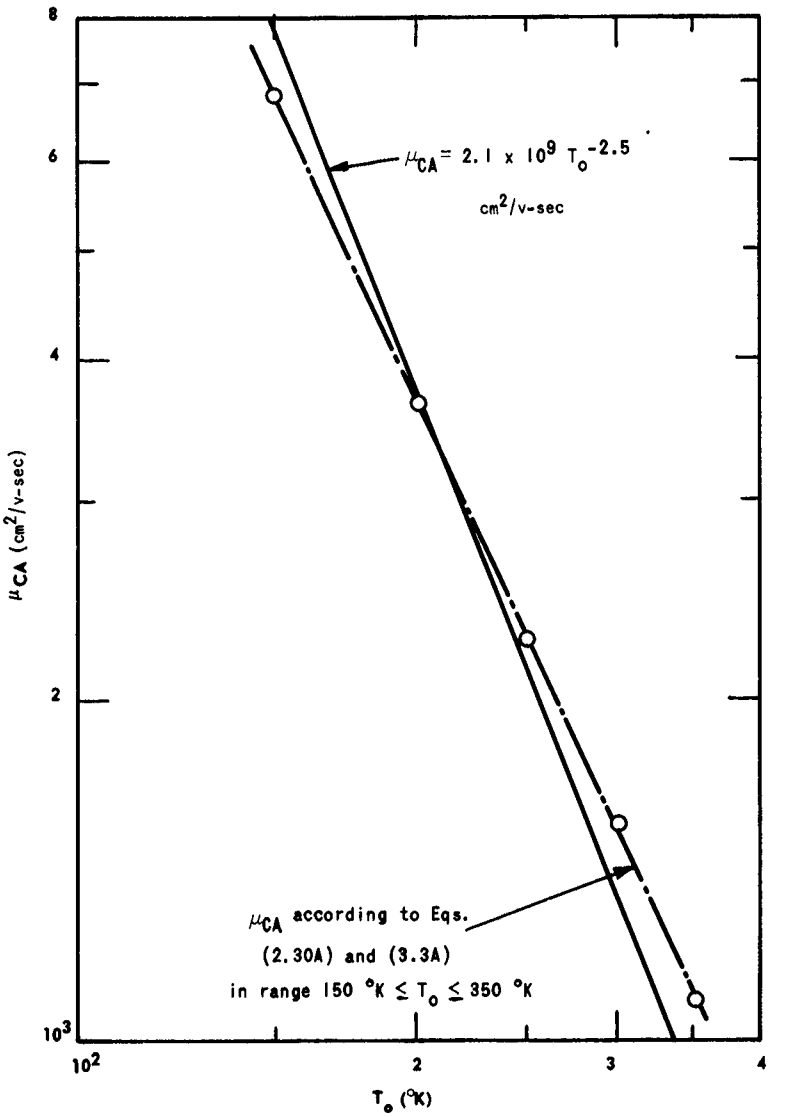

FIG. 11. FITTED, TEMPERATURE-DEPENDENT CURVE OF ZERO-FIELD ELECTRON MOBILITY TO n-TYPE SILICON WITH b = 3.16×10^3 cm^2/v-sec.

Using the values of μ_{aA}, μ'_{aA}, and μ_{oA} deduced in Eq. (3.3A), it is possible to evaluate F_1^2 from Eq. (2.42A). If we assume that the fitting of the temperature-dependent curve at zero field can be extrapolated down to 100 °K, then we may calculate the quadratic departure of electron mobility due to the applied field for both T_o = 99 °K and T_o = 300 °K. The results are listed in Table 1, and compared to Brown's experimental result[Ref. 26].

TABLE 1. EVALUATION OF F_1^2 AT VARIOUS LATTICE TEMPERATURES

T_o (°K)	$\frac{\mu_{aA}}{\mu'_{aA}}$	$\frac{\mu_{aA}}{\mu_{oA}}$	F_1^2 $(v/cm)^2$	
			Theoretical	Experimental
99	2.06	0.216	1.51×10^5	---
300	2.91	3.18	3.92×10^7	1.85×10^7

We can also evaluate the theoretical variation of drift velocity v with the applied field F by inserting the deduced values of μ_{aA}, μ'_{aA} and μ_{oA} into Eqs. (2.32A) and (2.33A). The best result is shown in Fig. 12 together with the experimental curve obtained by A. C. Prior [Ref. 25]. The result shows that the calculated, effective, electron temperature T is about six times higher than the estimated actual values at high field. The discrepancy between the theoretical evaluated values of v and the measured data is about 1.5.

TABLE 2. THE ESTIMATED MEAN ELECTRON ENERGY AND EFFECTIVE ELECTRON TEMPERATURE ASSOCIATED WITH THE POINTS MARKED ON THE THEORETICAL CURVE IN FIG. 12

Number of Point	Mean Electron Energy Estimated (ev)	Effective Electron Temperature (°K)
1	0.0267	310
2	0.0298	345
3	0.0414	480
4	0.0595	690
5	0.147	1700
6	0.298	3450
7	0.595	6900
8	1.490	17250

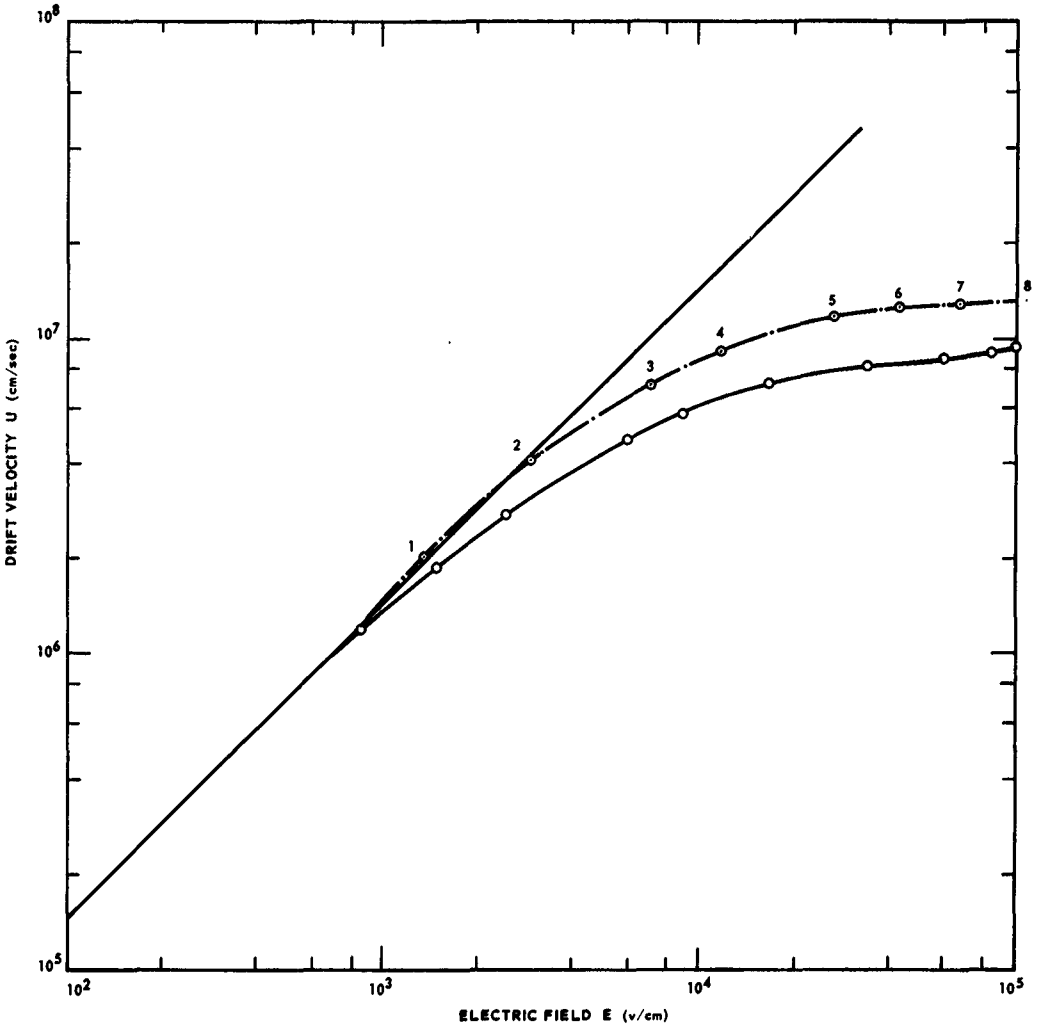

FIG. 12. THE VARIATION OF DRIFT VELOCITY WITH THE APPLIED FIELD FOR n-TYPE Si ACCORDING TO THEORY, TOGETHER WITH THE EXPERIMENTAL RESULT GIVEN BY PRIOR. Solid curve is Prior's data for 4.8 Ω-cm sample; broken curve is the best fit for the theoretical result. The estimated mean electron energy associated with the points marked is given in Table 2.

4. Discussion and Conclusion

The result which shows both discrepancies in the theoretical calculated electron temperature and drift velocity is not surprising. Since we oversimplify the physical picture implied in our formulations, there are at least some points which would influence the result to some extent. They are:

1. The form of distribution function: We assume the distribution function as the form of Eq. (1.1A) that is a Maxwellian distribution displaced in momentum space. We expand it in terms of spherical harmonics as shown in Eq. (1.2A) and cut off right after the second term. Obviously, it is oversimplified, especially for the case when the applied field is sufficiently high, while the distribution function may be far distorted from the quasi-equilibrium position. It is believed that this is extremely serious in the direction of the applied field, thus making the approximations used in the calculation breakdown.

2. The effective mass of the electrons in the conduction band: We assume the effective mass of the electrons in the conduction band to be constant through the calculation. Actually, this is not the case. The effective mass of the electrons in the conduction band is given by the relation

$$\frac{1}{m} = \frac{1}{\hbar^2} \nabla^2_{\vec{k}} E \ . \qquad (4.1A)$$

   According to the calculated band structure of silicon, it is clearly seen that the effective mass of the electron is actually a variable in the conduction band. This will certainly have some influence in the calculation.

3. The scattering mechanism of the energetic phonons near zone edge: The scattering mechanism of energetic phonons near zone edge is assumed to be of the same form as that of the energetic phonons at zone center. It seems quite reasonable to assume in this way as to distinguish from the different scattering mechanism due to the low energy, long-wavelength acoustic phonons. This assumption also makes it possible to evaluate $B(q)_i$, square of the interaction matrix. However, the theoretical justification is opened to question up to the present. If more information can be obtained from this kind of scattering mechanism, we may be able to establish a clearer physical model implied in the formulations.

4. The scattering mechanism involved between different minima in the conduction band: This is completely neglected in our formulation. However, if the applied field is sufficiently high as to make the electrons in the conduction band become hot, this kind of scattering may be able to occur. The energy minimum in <111> direction is about 0.39 ev higher than that in <100> direction in the conduction band of silicon, which is probably too high for this kind of scattering to occur even at high fields. (However, it is quite likely to occur in germanium since the energy minima in the <000> and <100> directions are only about 0.1 ev and 0.18 ev higher than that in the <111> direction [Ref. 20].)

5. Complication of band structure: The complication of band structure may result in different effective electron temperatures at the minima of different valleys and thus influence the final result.

The fitting of the theoretical calculation to the experimental result and the evaluation of the quadratic departure of electron mobility with the applied field shows that the scattering mechanism of the optical phonons is of great importance in the energy transfer processes from the electrons to the lattice, even when the mean electron energy is less than that of the optical phonons. This may be explained by the reason that even though the number of excited optical phonons is small, the energy transfer due to these excited optical phonons is much greater than that due to the low energy acoustic phonons.

Application of the theoretical calculation to n-type silicon shows that the results are still a factor of 6 higher in electron temperature and a factor of 1.5 higher in drift velocity than the accepted experimental results. (The result is even worse in n-type germanium, corresponding factors are 10 and 2 respectively.) This suggests that the distribution function and the scattering mechanism have to be considered in more detail.

However, comparison of the result obtained here to Stratton's (n-type Ge) clearly indicates that the method applied in our formulation results in almost saturation at the high field range; a result which is impossible to obtain if Stratton's method is applied. (The improvement in effective electron temperature is less than a factor of 2 in n-type Ge.)

REFERENCES

1. S. L. Miller, Phys. Rev., 105, 1957, p. 1246. Actually, Miller demonstrated only Eq. (3). Integration from W to O rather than O to W and interchanging α_n and α_p will transform (3) into (4).
2. "Solid-State Electronics," QSR No. 12, Signal Corps Contract DA36(039)SC85339, Stanford Electronics Laboratories, Stanford, Calif., 1 Jul to 30 Sep 1961.
3. J. L. Moll and R. Van Overstraeten, Solid State Electronics, 6, 1963, p. 147.
4. D. J. Bartelink, J. L. Moll, and N. I. Meyer, Phys. Rev., 130, 3 May 1963, p. 972.
5. G. A. Barroff, Phys. Rev., 128, 6, 15 Dec 1962, p. 2507.
6. E. Conwell, J. Phys. Chem. Solids, 8, Jan 1959, p. 234.
7. R. Stratton, Solid-State Physics I (Semiconductors), Part I., Academic Press, London, (1960), p. 343.
8. W. Shockley, Bell Syst. Techn. J., 30, 1951, p. 990.
9. E. J. Ryder, Phys. Rev., 90, 1953, p. 766.
10. J. B. Gunn, Progress in Semiconductors, 2, London, (1957), p. 213.
11. A. F. Gibson, J. B. Arthur, and J. W. Granville, J. Electronics, 2, 1956, p. 145.
12. H. Fröhlich, Proc. Roy. Soc., A, 188, 1947, p. 532.
13. H. Fröhlich and B. V. Paranjape, Proc. Phys. Soc., London, B 69, 1956, p. 21.
14. B. N. Brockhouse, Phys. Rev. Letters, 2, 1959, p. 256.
15. B. N. Brockhouse and P. K. Iyengar, Phys. Rev., 111, 1958, p. 747.
16. F. Seitz, Phys. Rev., 73, 1948, p. 549.
17. R. Stratton, Proc. Roy. Soc., A, 242, 1957, p. 355.
18. W. A. Harrison, Phys. Rev., 104, 1956, p. 1281.
19. C. Herring, Bell Syst. Tech. J., 34, 1954, p. 237.
20. F. Herman, I.R.E., 43, 1955, p. 1703.
21. D. P. Jenkins, Physica, 20, 1954, p. 967.
22. R. N. Dexter, H. J. Zeiger and B. Lax, Phys. Rev., 104, 1956, p. 637.
23. E. Ehrenreich and A. W. Overhauser, Phys. Rev., 104, 1956, p. 649.
24. G. W. Ludwig and R. L. Watters, Phys. Rev., 101, 1956, p. 1699.
25. A. C. Prior, J. Phys. Chem. Solids, 12, 2, 1960, p. 175.
26. M. A. C. S. Brown, J. Phys. Chem. Solids, 19, 1960, p. 218.

DISTRIBUTION LIST
for
FINAL REPORT
by
John L. Moll and Chun-Yuan Duh

under
Signal Corps Contract DA 36-039 SC-85339

No. of Copies	
	OASD (R&E), Rm 3E1065 The Pentagon Washington 25, D.C.
1	Attn: Technical Library
	Chief of Research & Development OCS, Department of the Army
1	Washington 25, D.C.
	Commanding General U.S. Army Electronics Command Fort Monmouth, New Jersey
1	Attn: AMSEL-AD
	Director U.S. Naval Research Lab. Washington, D.C.
1	Attn: Code 2027
	Commanding Officer & Dir. U.S. Navy Electronics Lab.
1	San Diego 52, California
	Commander Aeronautical Systems Div. Wright-Patterson AFB, Ohio
1	Attn: ASNXRR
	Commander A.F. Cambridge Res. Lab. L.G. Hanscom Field Bedford, Massachusetts
1	Attn: CRXL-R
	Commander A.F. Cambridge Res. Lab. L.G. Hanscom Field Bedford, Massachusetts
1	Attn: CRZC

No. of Copies	
	Commander Rome Air Development Center Griffiss AFB, New York
1	Attn: RAALD
	Commanding General U.S. Army Material Command Washington, D.C.
1	Attn: R&D Directorate
	Commander Defense Documentation Center Cameron Station, Bldg. 5 Alexandria, Virginia
10	Attn: TISIA
	Chief U.S. Army Security Agency Board Arlington Hall Station
2	Arlington 12, Virginia
	Deputy President U.S. Army Security Agency Board Arlington Hall Station
1	Arlington 12, Virginia
	Commanding Officer Harry Diamond Laboratories Connecticut Ave. & Van Ness St., N.W.
1	Washington 25, D.C.
	Commanding Officer U.S. Army Electronics Materiel Support Agency Fort Monmouth, New Jersey
1	Attn: SELMS-ADJ

No. of Copies	
	Director, USAEGIMRADA Fort Belvoir, Virginia
1	Attn: ENGGM-SS
	AFSC Scientific/Technical Liaison Office U.S. Naval Air Dev. Center
1	Johnsville, Pennsylvania
	Advisory Group on Electron Devices 346 Broadway, 8th Floor
3	New York, New York
	Marine Corps Liaison Office U.S. Army Electronics R&D Lab.
1	Fort Monmouth, New Jersey
	Commanding General U.S. Army Combat Dev. Command Fort Belvoir, Virginia
1	Attn: CDCMR-E
	Headquarters Electronic Systems Division L.G. Hanscom Field Bedford, Massachusetts
1	Attn: ESAT
	Philco Corporation C & Tioga Streets Philadelphia, Pennsylvania
1	Attn: Dr. C. Sutcliff
	Bell Telephone Laboratories Murray Hill, New Jersey
1	Attn: Dr. H. Loar
	Fairchild Semiconductor Corp. 545 Whisman Road Mt. View, California
1	Attn: Dr. R. Noyce
	Ohio State University 1314 Kinnear Road Columbus 8, Ohio
1	Attn: Dr. M.O. Thurston

No. of Copies	
	Rheem Semiconductor Corp. 327 Moffett Blvd. Mt. View, California
1	Attn: Dr. Leo Valdes
	Pacific Semiconductors, Inc. 10451 W. Jefferson Blvd. Culver City, California
1	Attn: Dr. J.W. Peterson
	Raytheon Company Research Division Waltham 54, Massachusetts
1	Attn: J.M. Lavine
	Lockheed Aircraft Corp. Missile Systems Division Sunnyvale, California
1	Attn: H.N. Leifer
	Lt. Col. William B. Lindsay Advanced Res. Project Agency Office Secretary of Defense
1	Washington 25, D.C.
	Hughes Products Semiconductor Division P.O. Box 278 Newport Beach, California
1	Attn: Technical Librarian
	Director, Monmouth Office U.S. Army Combat Dev. Command Communications-Electronics Agency
1	Fort Monmouth, New Jersey
	Mr. A.H. Young Code 618AIA Semiconductor Group Bureau of Ships Department of the Navy
1	Washington 25, D.C.
	Commanding Officer U.S. Army Electronics R&D Lab. Fort Monmouth, New Jersey
1	Attn: Director of Res/Eng.
1	Attn: Technical Doc. Center

No. of Copies	
	Commanding Officer U.S. Army Electronics R&D Lab. Fort Monmouth, New Jersey
1	Attn: Rpts Dist Unit, Solid State & Freq Cont Div (Record Cy)
1	Attn: Ch,S&M Br., Solid State & Freq Cont Div
1	Attn: Ch,M&QE Br., Solid State & Freq Cont Div
1	Attn: Dir.,Solid State & Freq Cont Div
1	Attn: W. Matthei, Solid State & Freq Cont Div
1	Attn: L. Heynick, Electron Tubes Division
5	Attn: A.P. LaRocque, Solid State & Freq Cont Div
	Total number of copies to be distributed - 60
	Chief of Naval Research Department of the Navy
1	Washington 25, D.C.
	Melpar, Inc. 3000 Arlington Blvd.
1	Falls Church, Virginia